Reprinted from INTERNATIONAL JOURNAL OF THERMOPHYSICS Vol. 9, No. 6, November 1988
Printed in Belgium

Experimental Apparatus for Measuring the Thermal Diffusivity of Pure Fluids at High Temperatures[1]

B. Kruppa,[2] P. Jany,[2] and J. Straub[2]

Dynamic light scattering represents a suitable method for measuring the thermal diffusivity of optically transparent fluids. The classic application of the method is the immediate vicinity around the critical point due to its dependence upon the intensity of scattered light and its high sensitivity to undesired light scattering. By means of subsequent modifications of the experimental setup, we have been able to expand this region of applicability over the last 12 years and could systematically investigate numerous substances and their binary mixtures within a temperature range of $280\ \mathrm{K} < T < 350\ \mathrm{K}$. Our planned investigation of fluids suitable for ORC-HP-technology necessitates performing measurements at higher temperatures and pressures. The experimental apparatus newly designed for this purpose is capable of sustaining a relatively high temperature constance at temperatures up to 700 K. Factors restricting the measurable range of state and their influence on the design of the sample cell are discussed.

KEY WORDS: critical region; light scattering; thermal diffusivity.

1. INTRODUCTION

Unsteady-state heat conduction can be determined by applying Fourier's law, in which thermal diffusivity, a, is the governing property of the substance:

$$a = \frac{\lambda}{\varrho c_p} \tag{1}$$

where λ, ϱ, and c_p denote the thermal conductivity, density, and specific isobaric heat, respectively.

[1] Paper presented at the Tenth Symposium on Thermophysical Properties, June 20–23, 1988, Gaithersburg, Maryland, U.S.A.

[2] Lehrstuhl A für Thermodynamik, Technische Universität München, Arcisstr. 21, D-8000 München 2, Federal Republic of Germany.

0195-928X/88/1100-0911$06.00/0

As opposed to equilibrium thermophysical properties, dynamic transport properties of fluids have not yet been sufficiently investigated. This is particularly the case in the range of state around the gas–liquid critical point, where a decreases rapidly due to the stong divergence of c_p, despite the lesser divergence in thermal conductivity λ. Moreover, the gradients with respect to ϱ and temperature T are exceptionally steep in this region.

Classical methods of determining transport properties such as thermal diffusivity a and thermal conductivity λ create temperature gradients within a medium through local heating. Methods such as the hot wire, the two concentric cylinders, or two parallel horizontal plates are suitable for this measurement. In the steady state, thermal conductivity ensues from the resulting temperature increase in the heating element; in the transient case, thermal diffusivity arises from the temporal propagation of the temperature front in the fluid. In the former instance, a can be calculated by applying Eq. (1), provided that an equation of state is available for determining ϱ and c_p.

These experimental techniques have been applied in different variations in the critical region of several fluids, namely, CO_2 [1], ^3He [2], ^4He [3], C_2H_6 [4], O_2 [5], H_2O [6], and NH_3 [7] for the determination of λ and CO_2 [8] for determining a. However, problems occur, due particularly to the appearance of undesired convection flows. Because of the strong increase in the thermal expansion coefficient in the region around the critical point and the resulting large Rayleigh number, even small temperature gradients suffice to induce convection. In addition, the superposition of a temperature gradient causes a change in the thermodynamic state of the fluid. This strong dependence of the thermal diffusivity upon T makes the realization of a temperature gradient which approaches zero desirable.

This aim can be achieved by using the relatively new method of dynamic light scattering or photon correlation spectroscopy. The fluid is in a state of thermodynamic equilibrium and the thermal diffusivity is derived from transport mechanisms in the microscopic scale. So far this method has been applied primarily in the close vicinity of the critical point, with SF_6 [9–12], CO_2 [13, 14], Xe [15], CH_4 [16], CH_3OH and CH_3ON [17], C_2H_6 [18], and NH_3 [19]. The measurements were typically carried out along the critical isochore and the coexistence curve and cover a temperature range around the critical point of about $0.001\ \mathrm{K} < |T - T_c| < 5\mathrm{K}$.

In our laboratory at the Technische Universität München, this range has been systematically extended to about 50 K. In addition, the dependence of a upon the density was investigated by taking measurements along several super- and subcritical isotherms. Numerous fluids have been investigated, namely, SF_6, CO_2, CHF_3, C_2H_6, N_2O, $CClF_3$, and Xe as

well as mixtures of the first three components [20–23]. It has been the aim of our research to determine the thermal diffusivity within a wide range of state around the critical point as systematically as possible and thus to be able to distinguish the specific influences of different substances. In this paper we describe our future activities as well as the necessary changes in the experimental setup.

2. SCOPE OF THE WORK

The restriction of the cited investigations [9–19] to the immediate vicinity around the critical point has two essential reasons. First, the method of measurement has several drawbacks, which become particularly noticeable with increasing distance from the critical point. Second, this approach originates from the desire to compare theoretical predictions with experimental results. Thus, a simple exponential dependence of certain thermophysical properties upon the reduce temperature difference,

$$\tau = \frac{T - T_c}{T_c} \tag{2}$$

is expected in the asymptotic region in the immediate vicinity of the critical point. For example [24],

$$c_p - c_v \sim |\tau|^{-\gamma} \tag{3}$$

where c_v denotes the specific isochoric heat, and [25]

$$\lambda - \lambda_B \sim |\tau|^{-\gamma+\nu} \tag{4}$$

where λ_B is the "background" component of the thermal conductivity, which is not influenced by the critical anomaly [26]. Thus, the newly defined "modified thermal diffusivity"

$$a^* = \frac{\lambda - \lambda_B}{\varrho(c_p - c_v)} \tag{5}$$

obeys the simple power law

$$a^* \sim \tau^{\nu} \tag{6}$$

along the critical isochore ($\varrho = \varrho_c$).

Since the relationships (3) and (4) are valid only for $|\tau| \to 0$, and the influence of c_v and λ_B as opposed to c_p and λ can be neglected within this region, a direct comparison of the τ dependence upon a with Eq. (6) is

possible. At further distances from the critical point, however, either c_v and λ_B have to be known or another law has to be established.

While dynamic light scattering represents a suitable method for determining a [Eq. (1)] in the close vicinity of the critical point, increasing problems arise at greater distances, which originate from the ability of the fluid to scatter incident light. The sufficient production of scattered light is an essential prerequisite for the applicability of the method. According to Ornstein–Zernike, the intensity of scattered light held at constant conditions (i.e., scattering angle, wavelength of light, intensity of incident light) can be determined as

$$I_s \sim \left(\frac{\delta\varepsilon}{\delta\varrho}\right)_T^2 \rho^2 \chi_T = I_{s,p} \tag{7}$$

where ε denotes the dielectric coefficient, and χ_T the isothermal compressibility. Figure 1 shows the factor of proportionality $I_{s,p}$ for five different fluids along the supercritical isotherm $\tau = 10^{-3}$ against ϱ/ϱ_c [27]. The figure clearly demonstrates the large decrease, of nearly five orders of magnitude, in $I_{s,p}$ from its maximum value at $\varrho/\varrho_c = 1$. Here the decrease in the region of lower densities is greater than at higher densities. All five fluids qualitatively exhibit the same behavior, with the tendency for Xe to be the strongest and SF_6 to be the weakest scattering medium.

Experimental examination into these regions of low light-scattering intensity requires special measures to be taken in the experimental setup, some of which are discussed in the next section.

The objectives behind the present work, as well as the selection of sub-

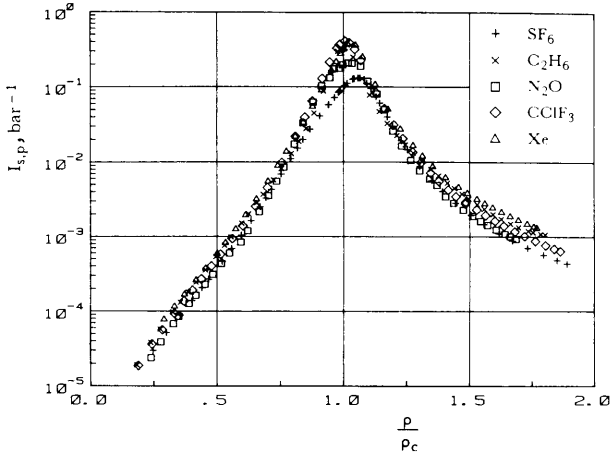

Fig. 1. Factor of proportionality of scattered light intensity along the supercritical isotherm $\tau = 10^{-3}$.

stances to be investigated, are characterized by their technical applicability. The necessity of finding, and systematically investigating, suitable working fluids for alternative heat-power processes was recognized at the VDI seminar "ORC-HP-Technology" held in 1984 in Zürich [28]. A research program was initiated by the Deutsche Forschungsgemeinschaft on a national level for this purpose. Our contributions are realized within the framework of this program. Despite its technical relevance to low-temperature energy conversion, the investigation of such fluids requires exceptionally high temperatures compared to conventional laboratory standards. Necessary changes in the experimental setup are also discussed in this context.

3. EXPERIMENTAL PROGRAM

In order to investigate systematically the expanded region around the critical point, measurements are made along two sub- and supercritical isotherms, respectively ($\tau = \pm 10^{-2}$ and $\tau = \pm 10^{-3}$), the critical isochore for $\tau > 0$, as well as both coexisting phases. The covered region of state, expressed in reduced density and pressure values, is $0.2 < \varrho/\varrho_c < 2.0$ and $0.4 < p/p_c < 3.0$, respectively. Measurements along $\varrho/\varrho_c = 1$ and along the coexistence curve cover the region of about $10^{-4} < |\tau| < 10^{-1}$. The corresponding absolute values are approximately

$$100 < \varrho < 1170, \qquad \rho \text{ in kg} \cdot \text{m}^{-3}$$

$$1.3 < p < 15, \qquad p \text{ in MPa}$$

$$275 < T < 540, \qquad T \text{ in K}$$

The group of halogenated hydrocarbons is particularly suitable as working fluids for use in ORC-HP processes. The substances we plan to investigate, along with their critical data, are listed in Table I. Aside from

Table I. ORC-HP Working Fluids to be Investigated

Substance		T_c(°C)	P_c(bar)	ϱ_c(kg · m^{-3})
R11	$CFCl_3$	198.0	43.7	555
R13	$CCLF_3$	28.8	38.60	581
R22	CHF_2Cl	96.0	49.36	525
R23	CHF_3	25.9	48.3	525
R113	$CFCl_2 \cdot CF_2Cl$	214.1	34.1	576
R114	$CF_2Cl \cdot CF_2Cl$	145.7	32.8	583
R142b	$C_2H_3F_2Cl$	137.05	41.23	435
R152a	$C_2H_4F_2$	113.5	44.9	365

thermal diffusivity measurements, other measured values are the temperature T, pressure p, and refractive index n. The density and isothermal compressibility can be derived from these data.

4. EXPERIMENTAL APPARATUS

The fundamental experimental setup has been described previously in Refs. 20 and 21. Thermal diffusivity is determined by using the homodyne technique of dynamic light scattering. An argon–ion laser, the power output of which can be varied within a range of 0.1 to 150 mW, serves as a light source. The scattered light is recorded at variable scattering angles which typically lie between 8 and 10°. A 96-channel digital correlator allows the setting of sample times down to 0.05 μs. In this paper, two selected aspects of the experimental setup are treated: restrictions of the method when approaching the immediate vicinity of the critical point and the design of a new test cell.

Restrictions in the applicability of the method of dynamic light scattering when approaching the critical point have several causes, most of which are dependent upon the geometry of the optical setup as well as that of the test cell. Since the presented experimental setup is strongly characterized by the requirement of performing measurements far from the critical point, and estimation of the closest attainable distance to the critical point becomes necessary. Several causes of these restrictions, as well as quantitatively attainable values of the reduced temperature difference τ are listed in Table II. In this case, the actual experimental boundary conditions were taken into account.

Explicit gravitational influence indicates the appearance of strong density gradients due to gravitation and large compressibility of the fluid.

Table II. Experimental Restrictions of the Method When Approaching the Critical Point

Limitation	Criterion	Minimal accessible τ
Gravitation (explicit)	1% change in χ_T	2.8×10^{-5} (vertical) 4.2×10^{-6} (horizontal)
Gravitation (implicit)	2.5% accuracy of a	3×10^{-5}
Multiple scattering	Low-turbidity Single scattering event	2.1×10^{-4} 1.7×10^{-4}
Hydrodynamic region	1% accuracy of a	1.5×10^{-4}
Laser heating	1% accuracy of τ	3×10^{-4}

This crucially influences measurements when χ_T varies considerably. The criterion for a 1% change in χ_T in the horizontal (3×10^{-4}m) and vertical (5×10^{-5}m) scale of the volume of observation was estimated using the calculations of Moldover et al. [29]. The dependence of the density (and thus thermal diffusivity) upon the height represents the implicit influence of gravity. If the height of critical density is determined to within $\pm 10^{-3}$ m, and accepting an error in a of $\pm 2.5\%$, the minimum accessible τ follows according to Kim et al. [30] as shown in Table II.

According to Moldover et al. [29], undesired multiple scattering of light along its optical path becomes possible when the product of the turbidity and the path length is of the order 1. Another criterion [31] predicts a single scattering event when the product of the wave vector and the correlation length is kept under 0.6. Both criteria lead to comparable results.

The hydrodynamic region, characterized by local thermodynamic equilibrium and a linear relationship between the thermal diffusivity and the decay rate, is attained when the product of the correlation length and the scattering vector becomes much smaller than 1. The use of corrective factors, derived from the "mode–mode-coupling" theory [32] allows for an estimation of the resulting error. Measuring at small scattering angles allows for smaller products. The power input due to the incident laser beam causes a local temperature increase of about 1 mK · mW^{-1} [33, 34]. Here a resulting increase in τ of 1% was employed as a criterion.

Summarizing, it can be assessed that all restrictive factors allow for a minimal accessible $|\tau|$ of about 1×10^{-4}.

The optimal determination of the sample-cell geometry is an important factor which directly affects the measurable range of state around the critical point. Measurements near the critical point require small sample-cell dimensions in order to minimize the above-mentioned multiple scattering and gravitational effects. On the other hand, a sufficient optical path length within the fluid and small scattering angles are essential to ensure adequate intensity of scattered light for measurements at distances farther from the critical point. Attaining small scattering angles, and thus reducing the scattering vector, also increases the maximum measurable value of thermal diffusivity [27]. In addition, a sufficient length of the sample cell is required in order to be able to isolate the scattered light originating in the scattering volume from that of the incident laser beam reflected off the quartz windows. This separation is achieved by means of a pinhole positioned in the immediate vicinity of the test cell. A cylindrical sample cell of 60-mm length and 34-mm diameter was selected as a reasonable compromise between these contradictory requirements, allowing for maximum scattering angles of $\pm 18°$.

In order to be able to achieve long-term temperature stability at temperatures above 400 K, an electrically heated test cell was devised, basically consisting of two thermally insulated heatable shells which can be controlled individually by computer (Fig. 2). The core of the apparatus is a stainless-steel sample cell, which is heat-shrunk into a larger copper cylinder. The copper cylinder and the two front flanges are seperately equipped with insulating heating wire and comprise the first heating circuit. This unit is mounted into a second protective cylindrical shell, merely leaving apertures for the transmitted laser beam and for registering the scattered light. This second heating circuit also contains three individual heating wires. To avoid large temperature gradients at the quartz windows of the sample cell arising from convection in the surroundings, the air in the vicinity of the windows is heated by a third circuit. These circuits are thermally insulated from each other so as to avoid control oscillations. Adjustable shields mounted over the apertures of the protective cylinder minimize the heat exchange to the surroundings. The entire apparatus is enclosed in a 0.1 m layer of insulation.

The temperature regulation of each heating circuit is achieved by computer-controlled voltage variation. For correcting the uneven temperature

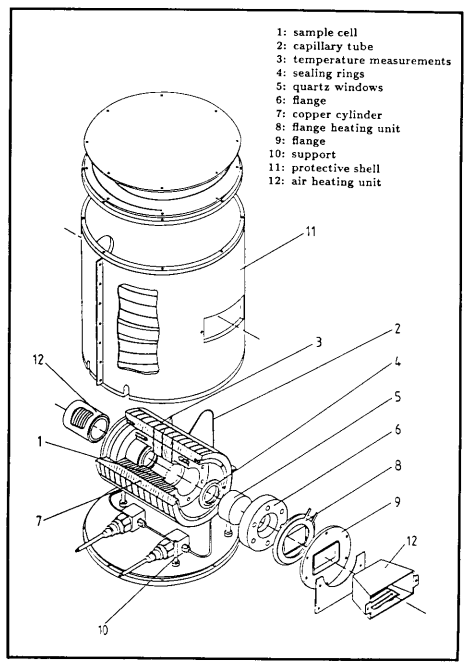

Fig. 2. Electrically heated test cell.

profile along the length of the sample cell or over the height of the entire apparatus (arising from increased heat through the quartz windows and onset of convection), the power input into a heating circuit can be split up among the individual heating elements. This is achieved by a pulse-width modulation of each element. Aside from the temperature regulation, measurements of the individual temperature and pressure data as well as the actual evaluations of thermal diffusivity are performed by personal computer. Its advantages over standard regulators are an increased versatility as well as the ability to adjust individual control parameters, thus optimizing control behaviour. Using this method of temperature regulation, we are able to achieve long-term temperature variations of under 0.01 K at 520 K. The apparatus was constructed to withstand temperatures and pressures of up to 700 K and 15 MPa, respectively.

The effective sealing of the sample volume poses a problem at higher temperatures, particularly when considering the temperature span of over 300 K covered by the thermal diffusivity measurements. Standard elastomere rings fail at such high temperatures, while rare-metal rings fail to accomplish satisfactory sealing over the entire temperature range due to differences in the thermal expansion coefficients of the materials used as well as an insufficient plastic deformation of the glass–metal sealing surface. We have therefore developed a sealing ring capable of fulfilling the necessary requirements of elasticity, durability, and deformability. The stainless-steel ring has a Y-shaped cross section and possesses a linear spring characteristic. The polished sealing surface has a width of only 0.5 mm, enabling high contact pressures. A thin foil of aluminium is placed between the ring and the glass/metal surface and is plastically deformed by the high pressures, resulting in a tight seal. Due to the cross-sectional form of the ring, the vapor pressure of the fluid increases the contact pressure and improves the quality of the seal with rising temperatures. There was no measurable leakage rate of the sample fluid within a temperature range of 0–250°C.

5. REPRESENTATIVE RESULTS

Figure 3 depicts measured thermal diffusivities a of the substance $CClF_3$ along the coexistence curve and isotherms against the reduced density ϱ/ϱ_c. These representative results qualitatively conform with data for other substances. The accuracy of the thermal diffusivity measurements is estimated to be better than 2% in a range over nearly four orders of magnitude.

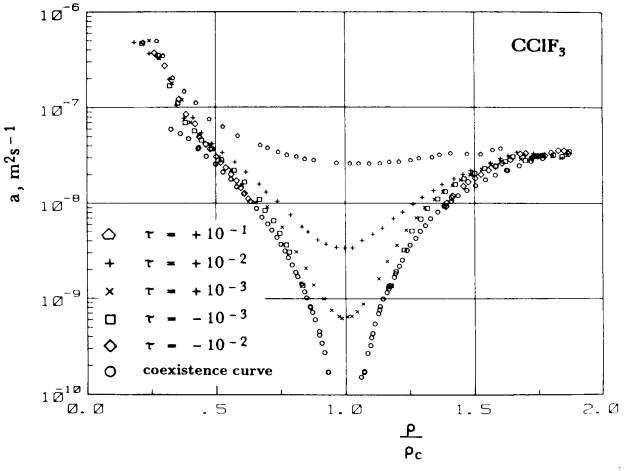

Fig. 3. Measured thermal diffusivities of $CClF_3$ along the coexistence curve and several isotherms.

6. CONCLUSION

The experimental apparatus presented in this paper is capable of measuring thermal diffusivities of pure fluids within a wide region around the critical point. This region, characterized by restrictions limiting measurements in the immediate vicinity of, and at distances farther from, the critical point can be described by $0.02\ \text{K} < |T - T_c| < 50\ \text{K}$. Using the experimental results of a selected fluid, the applicability of the method was demonstrated. The investigation of new working fluids suitable for ORC-HP processes into region of higher temperatures and pressures requires extensive modification of the apparatus. A newly designed test cell capable of withstanding temperatures and pressures of up to 700 K and 15 MPa respectively, was presented.

ACKNOWLEDGMENT

The present authors would like to express their gratitiude to the Deutsche Forschungsgemeinschaft (DFG) for supporting this research project.

REFERENCES

1. A. Michels, J. V. Sengers, and P. S. Van der Gulik, *Physica* **28**:1216 (1962).
2. C. E. Pittman, L. H. Cohen, and H. Meyer, *J. Low Temp. Phys.* **46**:115 (1982).

3. A. Acton and K. Kellner, *Physica* **103B**:212 (1981).
4. R. C. Prasad and J. E. S. Venart, *Int. J. Thermophys.* **5**:367 (1984).
5. L. A. Weber, *Int. J. Thermophys.* **3**:117 (1982).
6. R. Tufeu and B. Le Neindre, *Int. J. Thermophys.* **8**:283 (1987).
7. R. Tufeu, D. Y. Ivanov, Y. Garrabos, and N. Le Neindre, *Ber. Bunsenges. Phys. Chem.* **88**:442 (1984).
8. H. Becker and U. Grigull, *Wärme- Stoffübertragung* **11**:9 (1978).
9. N. C. Ford and G. B. Benedek, *Phys. Rev. Lett.* **15**:649 (1965).
10. G. B. Benedek, *French Phys. Soc.* **49** (1969).
11. P. Braun, D. Hammer, W. Tscharnuter, and P. Weinzierl, *Phys. Lett. A* **32**:390 (1970).
12. G. T. Feke, J. B. Lastovka, G. B. Benedek, K. H. Langley, and P. B. Elterman, *Opt. Comm.* **7**:13 (1973).
13. H. L. Swinney and H. Z. Cummins, *Phys, Rev.* **171**:152 (1968).
14. B. Maccabee and J. A. White, *Phys. Rev. Lett.* **27**:495 (1971).
15. D. L. Henry, H. L. Swinney, and H. Z. Cummins, *Phys. Rev. Lett.* **25**:1170 (1970).
16. B. J. Ackerson and G. C. Straty, *J. Chem. Phys.* **69**:1207 (1978).
17. W. Grabner, F. Vesely, and G. Benesch, *Phys. Rev. A* **18**:2307 (1978).
18. R. F. Chang and T. Doiron, *Proc. 8th Symp. Thermophys. Prop., Vol. 1*, J. V. Sengers, ed. (Am. Soc. Mech. Eng., New York, 1982), p. 458.
19. R. Tufeu, A. Letaief, and B. Le Neindre, *Proc. 8th Symp. Thermophys. Prop., Vol. 1*, J. V. Sengers, ed. (Am. Soc. Mech. Eng., New York, 1982), p. 451.
20. E. Reile, P. Jany, and J. Straub, *Wärme- Stoffübertragung* **18**:99 (1984).
21. P. Jany and J. Straub, *Int. J. Thermophys.* **8**:165 (1987).
22. P. Jany and J. Straub, *Chem. Eng. Comm.* **57**:67 (1987).
23. E. Reile and J. Straub, *Proc. 8th Symp. Thermophys. Prop., Vol. 1*, J. V. Sengers, ed. (Am. Soc. Mech. Eng., New York, 1982), 463.
24. J. V. Sengers, *Ber. Bunsenges. Phys. Chem.* **74**:234 (1972).
25. L. P. Kadanoff and J. Swift, *Phys. Rev.* **166**:89 (1968).
26. J. V. Sengers and P. H. Keyes, *Phys. Rev. Lett.* **26**:70 (1971).
27. P. Jany, *Die Temperaturleitfähigkeit reiner Fluide im weiten Zustandsbereich um den kritischen Punkt*, Thesis (Technical University Munich, Munich, 1986).
28. VDI-Gesellschaft Energietechnik, *ORC-HP-Technology* (VDI-Verlag, Düsseldorf, 1984).
29. M. R. Moldover, J. V. Sengers, R. W. Gammon, and R. J. Hocken, *Rev. Mod. Phys.* **51**:79 (1979).
30. D. M. Kim, D. L. Henry, and R. Kobayashi, *Phys. Rev. A* **10**:1808 (1974).
31. C. M. Sorensen, R. C. Mockler, and W. J. O'Sullivan, *Phys. Rev. A* **16**:365 (1977).
32. K. Kawasaki, *Ann. Phys.* **61**:1 (1970).
33. C. M. Sorensen, R. C. Mockler, and W. J. O'Sullivan, *Phys. Rev. Lett.* **40**:777 (1978).
34. H. C. Burstyn and J. V. Sengers, *Phys. Rev. A* **27**:1071 (1983).

Printed by Catherine Press, Ltd., Tempelhof 41, B-8000 Brugge, Belgium